

L.I. Markaszowa, W.D. Poznjakow, E.N. Berdnikowa

Effect of Welding Parameters on the Structure, Mechanical Properties and Crack Resistance of Welded Joints Made of Steel 14HGN2MDAFB

Abstract: The article presents test results concerning the structure and the phase composition of the weld and HAZ metal of welded joints made of high yield point (above 700 MPa) steel 14HGN2MDAFB using the mechanised welding method. The tests involved the analytical assessment of the effect of structural parameters on the mechanical properties (R_e , K_{IC}^*) of welded joints as well as the determination of the role of structural factors (phase composition, grain structure, subgrain structure and dislocation) in terms of changes in local internal stresses (τ_j), i.e. crack formation concentrators. The tests enabled the identification of optimum technological conditions ensuring the obtainment of high quality and reliable welded joints of structures characterised by high mechanical properties and crack resistance.

Keywords: high strength steel, steel 14HGN2MDAFB, welding parameters

DOI: [10.17729/ebis.2018.2/5](https://doi.org/10.17729/ebis.2018.2/5)

In the machine-building industry, high strength steels are commonly used in the fabrication of welded structures of extension arms, moving cranes, concrete-pumping pumps etc. The use of high strength steels makes it possible to reduce the weight of the above-named structures and improve their technical characteristics. The aforesaid structures are usually fabricated using gas-shielded mechanised or automated welding. Appropriate welding conditions should provide both high efficiency and desired complex of mechanical properties of the weld metal and the heat affected zone (HAZ), including their high cold crack resistance.

Mechanical properties and the cold crack resistance of welded joints made of high strength steels are known to be significantly affected by

the structure of the weld metal and that of the HAZ. The formation of the structure in the HAZ metal affected by welding thermal cycles is well known [1-4] and supported by experimentally obtained information concerning the transformation of the structure of the weld and that of the HAZ in welded joints made of steels having a yield point of 600 MPa (17H2M, 10G2FB and others) in relation to a cooling rate ($W_{6/5} \approx 2.5 \dots 20^\circ\text{C/s}$), fixing rigidity, the use of alloying agents (10HN2GSMFTJu, 08G2S, 08H20N9G7T) and exposure to external loads (static, dynamic, cyclical) [5-8]. The authors used related structural and analytical assessments to forecast possible methods enabling the improvement of mechanical characteristics of welded joints and increasing their crack resistance by providing the

L.I. Markaszowa, W.D. Poznjakow, E.N. Berdnikowa – E. O. Paton Electric Welding Institute, the National Academy of Sciences of Ukraine, Kiev

appropriate phase composition and parameters of a forming structure. However, today's industry increasingly often requires the use of high strength steels having a yield point of 700 MPa and higher, characterised by high toughness, plasticity and brittle crack resistance. Unfortunately, as regards the above-named steels, the effect of technological welding conditions on the structure and mechanical properties of the weld metal and the HAZ of joints made under rigid fixing conditions has not been sufficiently investigated.

In view of the foregoing, this research work aimed to examine the effect of technological conditions of mechanised welding on structural and phase transformations as well as to assess the effect of structural factors on the mechanical properties and crack resistance of rigidly fixed welded joints made of high strength steel having a yield point exceeding 700 MPa.

Materials and Methodology

The tests involved 8 mm thick butt welded joints made of high strength steel 14HGN2MDAFB (0.183% C; 1.19% Cr; 0.98% Mn; 2.07% Ni; 0.22% Mo 0.08% V; 0.33% Si; below 0.018% P and 0.005% S), fixed rigidly, using solid wire Sv-10HN2GSMFTJu ($\leq 0.1\%$ C; 0.7% Cr; 0.4% Mn; 0.22% Mo; 0.15% V; 0.24% Si; 0.007% S). Welding conditions involved a welding current of 220–240 A; an arc voltage of 30–32 V as well as welding rate $vW \approx 5$ mm/s; 8 mm/s; 11 mm/s and 14 mm/s (18 m/h; 30 m/h; 40 m/h and 50 m/h respectively). The above-presented welding parameters made it possible to cool the HAZ metal within the temperature range of 600 to 500°C at rate $W_{6/5}$ amounting approximately to 10–12°C/s; 19–22°C/s; 25–28°C/s and 38°C/s, respectively.

Tests concerning structural and phase transformations as well as changes in the chemical composition, the manner of distribution and the density of crystallographic lattice defects in the weld metal and the HAZ of welded joints were performed using various experimental methods

applied in today's metallurgy, including optical metallography (Versamet-2 and Neophot-32 microscopes), raster electron microscopy (SEM 515, PHILIPS) and transmission electron microscopy (JEM-200CX, JEOL). Hardness was measured using an M-400 microhardness tester (Leco) under a load of 0.98 N (0.1 kG).

Test Results and Analysis

Presented below are test results concerning phase constituents formed in the weld metal and in the HAZ, i.e. ferrite (F); upper bainite (B_g), lower bainite (B_d) and martensite (M) as well as their volumetric content (V , %), grain size (D_{gr}) and related changes in microhardness (HV).

In relation to the minimum welding rate amounting to 5 mm/s the weld metal structure was ferritic-bainitic ($F-B$) with the dominant formation of upper bainite structures ($V = 65\%$) where $D_{gr} = 50 - 200 \times 200 - 700 \mu\text{m}$ and $HV(F-B) = 2850 - 2940$ MPa (Fig. 1a, Fig. 2a). Along the fusion line on the weld side, in the presence of the clear arrangement of columnar crystallites, microhardness increased to $HV(F-B) = 3140 - 3360$ MPa, and, on the HAZ side, to $HV = 3660 - 3830$ MPa. The HAZ metal in the superheating area (HAZ area no. I) was characterised by the bainitic-martensitic structure ($B-M$), grain refinement $D_{gr} = 40 - 100 \mu\text{m}$ and a 30% increase in microhardness to $HV(B-M) = 3660 - 4010$ MPa (Fig. 1b, Fig. 2c). In the area of recrystallization (HAZ area no. II) and in the area of incomplete recrystallization (HAZ area no. III) the structure underwent refinement (4 – 6 times in comparison with the superheating area) and microhardness amounted to $HV = 3660 - 3830$ MPa (Fig. 1c, d). The metal in the recrystallization area was characterised by the ferritic-bainitic structure (in relation to $HV = 2970 - 3660$ MPa).

However, in the superheating area (HAZ area no. I) of the welded joint obtained using a welding rate of 5 mm/s, near the fusion line, a cold crack was formed (indicated using arrows in Figure 1e) and a failure followed.

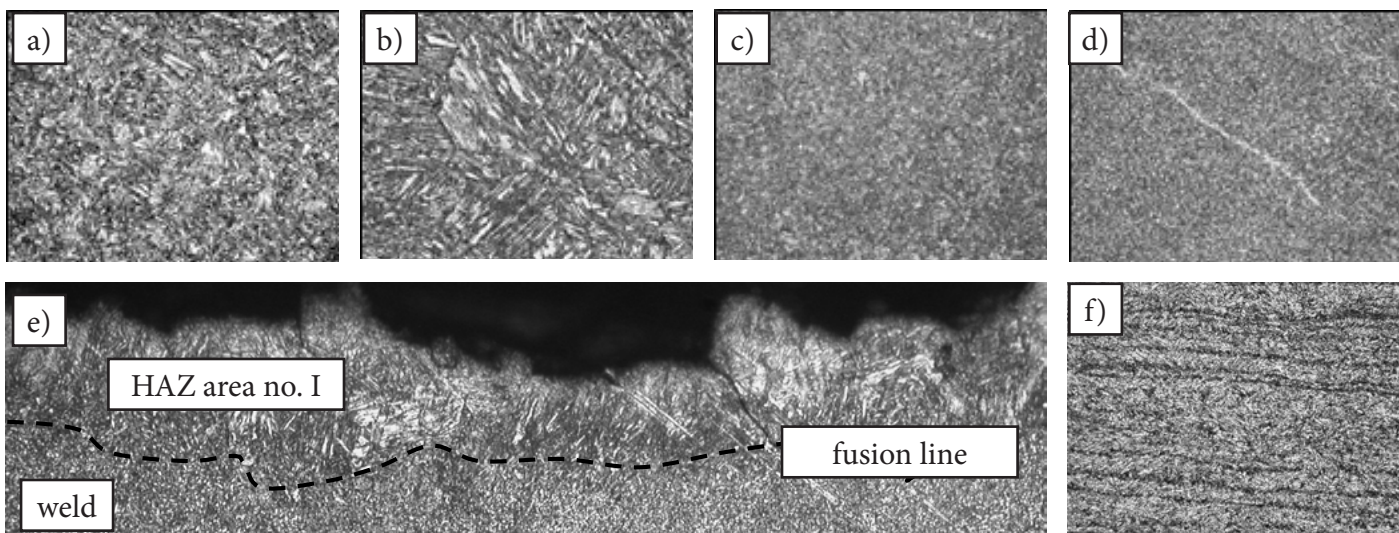


Fig. 1. Microstructure of the weld metal (a); HAZ area no. I (b); HAZ area no. II (c); HAZ area no. III (d); crack zone (e) and base material (f), $v_w = 5 \text{ mm/s}$, $\times 500$

In relation to all of the applied welding conditions (5 – 14 mm/s) the structure of the base material of steel 14HGN2MDAFB was identical, bainitic-ferritic (B-F), characterised by grain size $D_{gr} = 15 - 25 \mu\text{m}$ and microhardness $HV(B-F) = 2990 - 3510 \text{ MPa}$ (Fig. 1f.)

Therefore, where $v_w = 5 \text{ mm/s}$, the metal of the welded joints contained the coarse-grained and highly graded structure of, primarily, upper bainite. The phase composition of the metal changed from ferritic-bainitic (weld, i.e. the area of recrystallisation) to bainitic-martensitic (HAZ, i.e. the area of superheating).

The increase in a welding rate to 8 mm/s was accompanied by the refinement (on average by 1.8 times) of the weld structure (in comparison with the outcome obtained using a welding rate

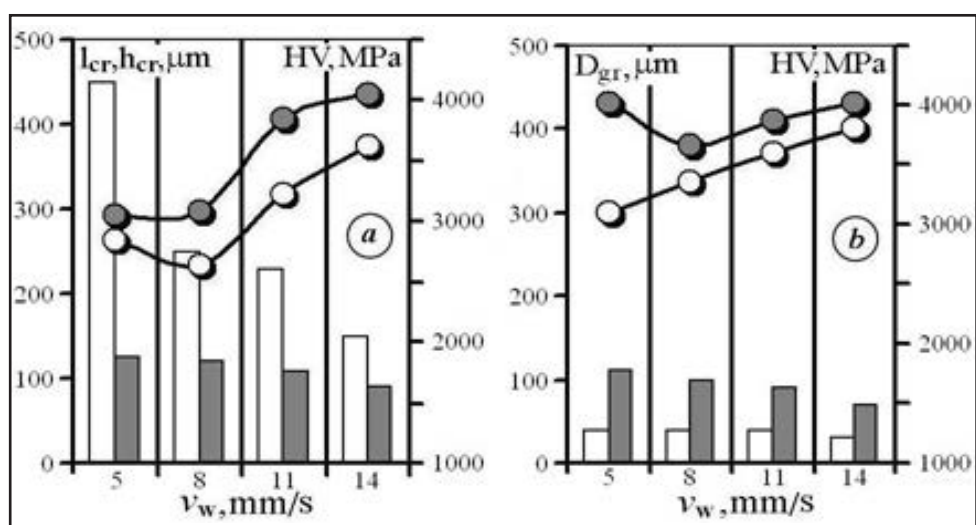


Fig. 2. Change in the average size of structural parameters, i.e. crystallites (■ - h_{cr} ; □ - l_{cr}), grain (D_{gr} - □/■ - min/max) and microhardness (HV - ○/● - min/max) in the weld metal (a) and HAZ (b) of the welded joints in relation to welding rates

of 5 mm/s) as well as by a decrease in the upper bainite content both in the weld (to $V = 50\%$) and in the HAZ (to $V = 30\%$) (Fig. 3).

When the welding rate amounted to 11 mm/s, the metal of the welds and HAZ of the welded joints contained primarily lower bainite ($V = 45\%$ and 60% , respectively) (Fig. 4). In comparison with the joints made using welding rate

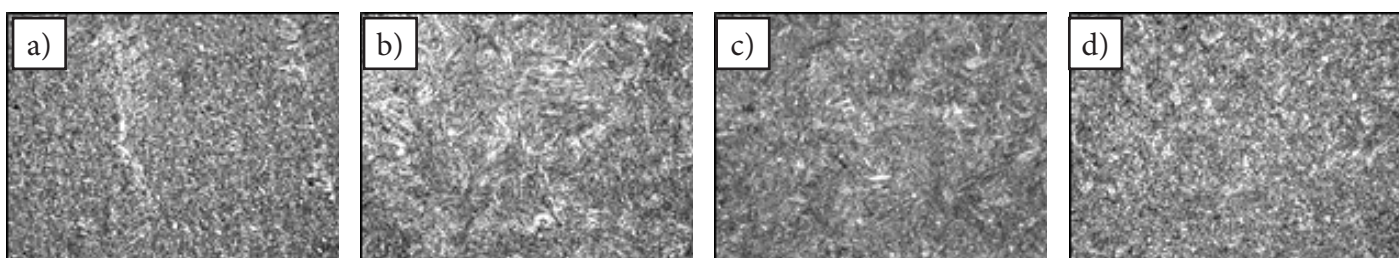


Fig. 3. Microstructure of the weld metal (a); HAZ area no. I (b); HAZ area no. II (c); HAZ area no. III (d); $v_w = 8 \text{ mm/s}$, $\times 500$

$v_w = 5$ mm/s, the above-named case was related to the change in the phase composition, the refinement of the grain structure (2-3 times) and the relatively uniform microhardness in the weld and HAZ.

As can be seen, the increase in a welding rate from 5 mm/s to 14 mm/s led to the change in the phase composition of the weld metal from ferritic-bainitic to bainitic-martensitic, a 30% increase in microhardness without its gradients and to the formation of a more equiaxial granular structure (refined 2-3 times) in the welding zone. In the HAZ superheating area, the phase composition was bainitic-martensitic regardless of welding rates applied, where the greatest microhardness gradients (1.3 times) occurred where the minimum welding rate of 5 mm/s was used. The coarse-grained structures with high gradients, primarily of upper bainite could lead to the non-uniform level of mechanical properties and a significant decrease in crack resistance.

It was ascertained that the uniform structural changes in the phase composition and the optimum structure of the test welded joints (in terms of the refinement of structural parameters, the lack of gradients along the grain structure and microhardness) were formed when the welding rate amounted to 11 mm/s. The

foregoing should provide uniform mechanical properties in the welding zone (weld, fusion line, HAZ), favour the optimum combination of mechanical and plastic properties and of ductility as well as prevent the formation of crack initiators.

The tests of the subtle structure involved the welded joints with the most significant (in terms of crack resistance) structural and phase transformations, i.e. parameters related to $v_w = 5$ mm/s (gradient structure) and $v_w = 11$ mm/s (optimum structure).

The detailed tests were focused on the following parameters of the subtle structure: changes in density (ρ) and dislocation distribution in various structural elements (inside and along boundaries of structural components), the nature of a forming substructure, the width of the laths (h_p) of bainitic (B) and martensitic (M) constituents, effective distances between carbide phases (λ_u), (see Table 1).

In relation to a welding rate of 5 mm/s, the weld metal along grain boundaries, primarily along the boundaries of upper bainite (B_g), contained extended dislocation pile-ups in area $\rho = 1 - 2 \times 10^{11} \text{ cm}^{-2}$, which, in cases of such structural elements, translates into the high gradient of dislocation density (Fig. 6a). The increase in the welding rate from 5 mm/s to 11 mm/s

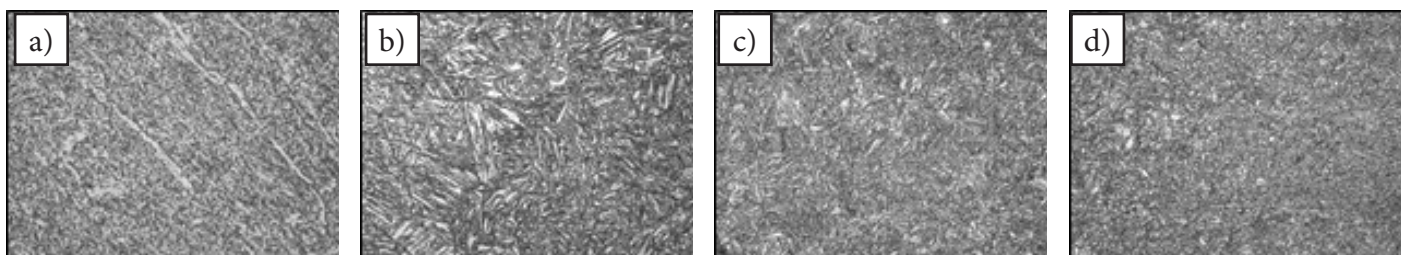


Fig. 4. Microstructure of the weld metal (a); HAZ area no. I (b); HAZ area no. II (c); HAZ area no. III (d); $v_w = 11$ mm/s, $\times 500$

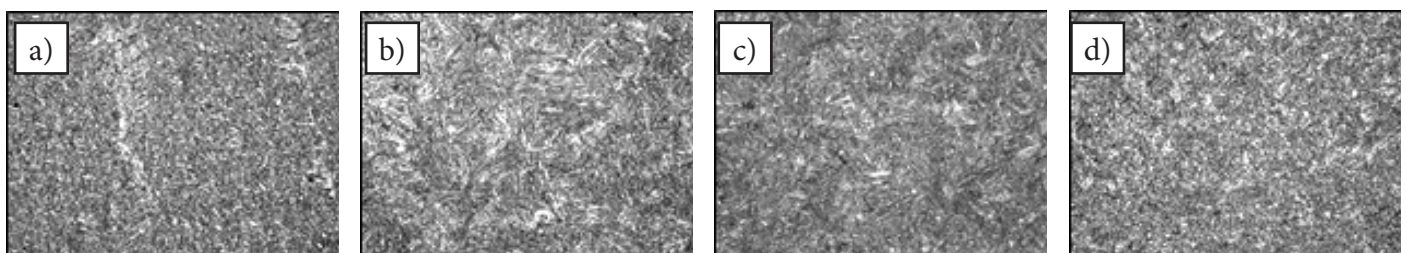


Fig. 5. Microstructure of the weld metal (a); HAZ area no. I (b); HAZ area no. II (c); HAZ area no. III (d); $v_w = 14$ mm/s, $\times 500$.

combined with the fragmentation (fragments size $d_{fr} = 0.4 - 0.5 \mu\text{m}$) of the lower bainite structure (B_d) in the weld metal resulted in the relatively uniform volumetric distribution of dislocation density ($\rho = 4 - 6 \times 10^{10} \text{ cm}^{-2}$) (Fig. 6b). Area I of the HAZ was characterised by a certain increase in the above-named dislocation density (up to $\rho = 6 - 8 \times 10^{10} \text{ cm}^{-2}$) (Fig. 6c).

Therefore, the increase in the welding rate to 11 mm/s was accompanied by the change in the phase composition of the structural constituents of the metal in each zone of the welded joint. The content of upper bainite and martensite decreased, the volumetric content of fragmented lower bainite increased (2 to 4 times) (Fig. 6c), which, in turn, eliminated the gradients of dislocation density in the above-named structure and was likely to provide both uniform strength and high crack resistance of welded joints.

The mechanical test results involving specimens, i.e. rigid welded joints, revealed that the highest tensile strength ($\sigma_{ult} = 930 - 1171 \text{ MPa}$) was that of the welds made when $v_w = 11 \text{ mm/s}$ (Fig. 7a). Slightly lower values were related to $v_w = 14 \text{ mm/s}$ and $v_w = 8 \text{ mm/s}$, i.e. $\sigma_{ult} = 883 - 908 \text{ MPa}$ and $\sigma_{ult} = 786 - 861 \text{ MPa}$, respectively. The mechanical tests did not involve the welded joints made using a minimum welding rate of 5 mm/s as they contained cold cracks (Fig. 1e).

Table 1. Parameters of the subtle structure of the welded joints

v_w		5 mm/s		11 mm/s	
		Weld	HAZ area no. I	Weld	HAZ area no. I
$h_p, \mu\text{m}$	B_d	0.50...1.0	0.40...0.80	0.40...0.80	0.40...0.60
	B_g	0.80...1.20	0.50...0.90	0.60...1.20	0.50...0.80
	M	0.70...1.70	0.70...1.50	0.70...1.40	0.80...1.0
$\lambda_{\psi}, \mu\text{m}$	B_d	0.06...0.08	0.05...0.08	0.06...0.08	0.05...0.08
	B_g	0.60...1.0	0.40...0.60	0.50...1.0	0.4...0.70
	M	0.04...0.10	0.04...0.10	0.04...0.10	0.04...0.10

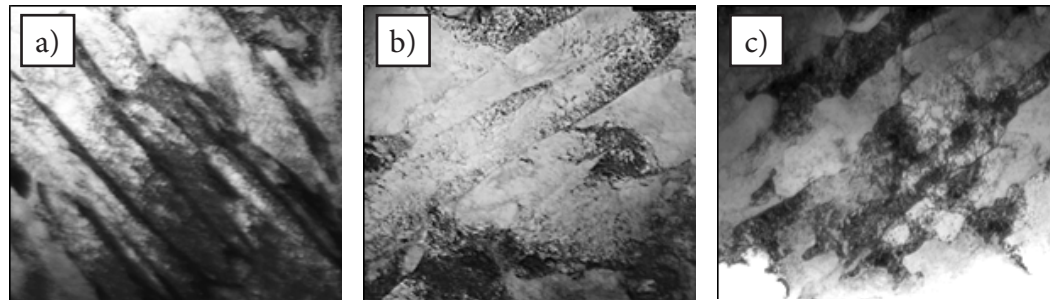


Fig. 6. Microstructure of upper (a) and lower (b, c) bainite in relation to a welding rate of : a – 5 mm/s; b, c – 11 mm/s; $\times 20000$

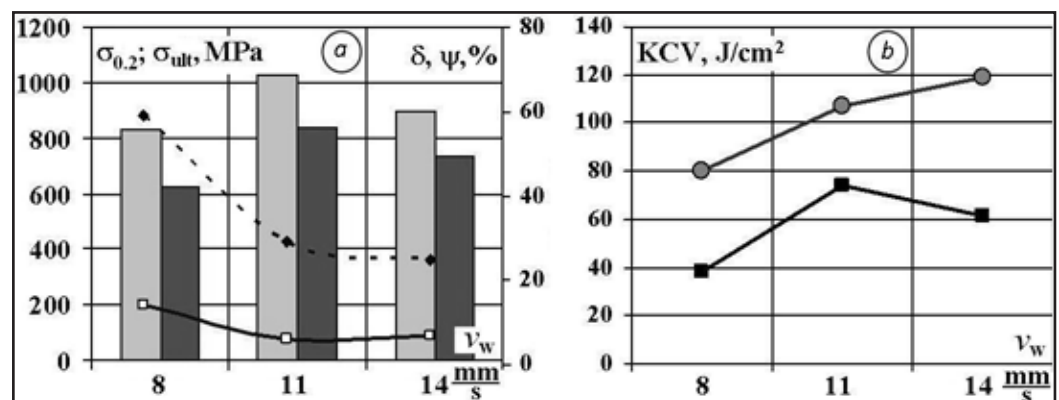


Fig. 7. Mechanical test results – \square tensile strength; \blacksquare yield point; \square relative elongation; \blacklozenge relative area reduction – (a) and the toughness (\bullet – KCV^{+20} ; \blacksquare – KCV^{-40}) of welds (b) made using various welding rates

The results of the impact strength tests performed at a test temperature T_{ISP} restricted within the range of $+20^\circ\text{C}$ to -40°C revealed that the lowest toughness values ($\text{KCV}^{-40} = 38.4 \text{ J/cm}^2$ at $T_{ISP} = -40^\circ\text{C}$) were those of the welds made when $v_w = 8 \text{ mm/s}$ (Fig. 8b). The highest toughness values ($\text{KCV}^{-40} = 73.9 \text{ J/cm}^2$) were those of the welded joints made when $v_w = 11 \text{ mm/s}$. Slightly lower values ($\text{KCV}^{-40} = 61.6 \text{ J/cm}^2$) were observed in the welds made using welding rate $v_w = 14 \text{ mm/s}$.

The above-presented tests demonstrated the effect of technological welding conditions

on mechanical properties of welded joints. The foregoing was related to the features of a forming structure and the phase composition of the metal.

The results of the fractographic tests of the specimens after the impact strength tests enabled the comparison of weld metal cracking nature along crack zones in relation to a test temperature.

For $T_{ISP} = +20^{\circ}\text{C}$ in relation to a welding rate restricted within the range of 8 to 14

mm/s, the microrelief of the crack surface was characterised by a ductile type crack. In relation to $T_{ISP} = -40^{\circ}\text{C}$, the increase in the welding rate from 8 mm/s to 11 – 14 mm/s increased, on average by twice, the width of the ductile crack zone in the area of the notch, side scarfs and fracture. In turn, in the arterial crack zone, the above-named increase in the welding rate was responsible for the decrease in the volumetric content of brittle intergranular split-off by 10 – 20% (Fig. 8). In addition, it was possible to observe the refinement of brittle crack facets (from 50 – 70 μm to 30 – 50 μm) and the decrease in the length of secondary cracks (from 3.0 – 6.0 μm to 5 – 15 μm) along the boundaries of structural constituents, characteristic of higher resistance to arterial crack development (Fig. 8b, c). The highest toughness indicators ($KCV^{-40} = 73.9 \text{ J/cm}^2$) were obtained in relation to a welding rate of 11 mm/s (Fig. 7b).

In the joint made using welding rate $v_w = 5 \text{ mm/s}$, i.e. where a cold crack was formed, the crack was formed in the HAZ grain growth area near the fusion line (Fig. 9a). In the

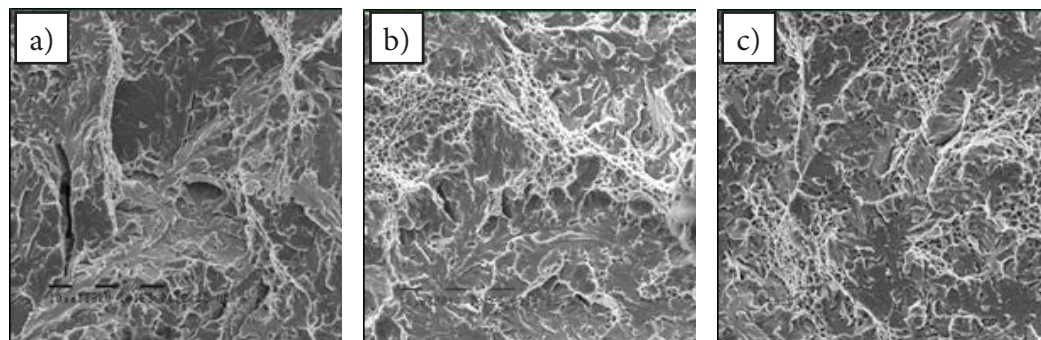


Fig. 8. Microstructure of the fracture in the zone of the arterial crack of welded joints ($T_{ISP} = -40^{\circ}\text{C}$) made using various welding rates, i.e. a: 8 mm/s; b: 11 mm/s; c: 14 mm/s; $\times 1010$

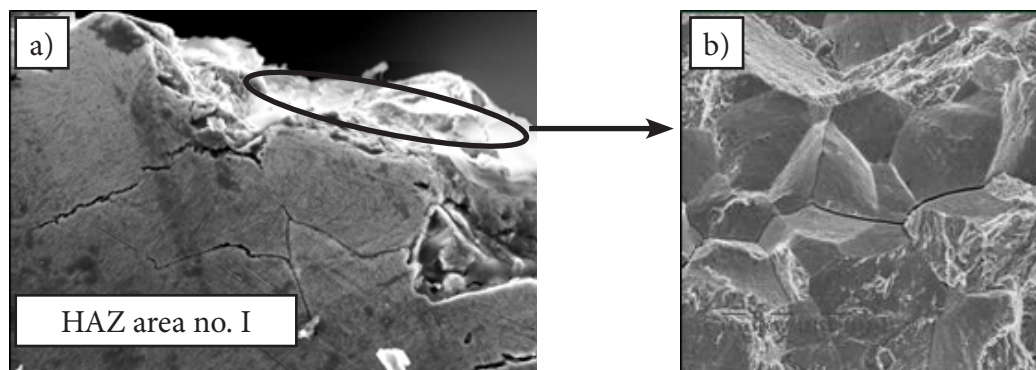


Fig. 9. Welded joint microstructure in the crack zone (a) and the surface of the fracture (b), $\times 1010$, $v_w = 5 \text{ mm/s}$.

above-named case, the crack was of brittle intragranular nature with secondary cracking along grain boundaries (Fig. 9b).

Test results obtained in relation to various structural levels (from granular to dislocation) enabled analytical assessments of the specific (diversified) effect of individual structural-phase factors and parameters (phase composition, grain size, subgrain, dislocation density etc.) on the change in the total (integral) size of mechanical properties ($\sigma_{0,2}$), brittle crack resistance (K^*_{1C}) and local internal stresses (τ_j), being sources of propagation, as well as on the development of cracks in tested structural micro-areas [7-9] (Fig. 10 – 12).

It was assumed that value σ_T was the sum of a series of components, i.e. $\Sigma\sigma_T = \Delta\sigma_0 + \Delta\sigma_{S,S} + \Delta\sigma_G + \Delta\sigma_{SG} + \Delta\sigma_D + \Delta\sigma_{D,H}$. In accordance with the equation including well-known Hall-Petch, Orowan etc. relations [9-13], where $\Delta\sigma_0$ – metal lattice resistance during the displacement of free dislocations (tension of lattice friction or the Peierls-Nabarro stress); $\Delta\sigma_{S,S}$ – solid solution hardening obtained using alloying components

and additives (hardening in the solid state); $\Delta\sigma_G$, $\Delta\sigma_{SG}$ – hardening through changes in the grain and subgrain sizes in accordance with the Hall-Petch relation (hardening of grain boundaries and substructural hardening); $\Delta\sigma_D$ – dislocation hardening triggered by inter-dislocation effect; $\Delta\sigma_{D.H.}$ – hardening by dispersive particles according to Orowan (dispersion hardening).

Calculated values of brittle crack resistance K^*_{IC} were determined using dependence [14]: $K^*_{IC} = (2E \cdot \sigma_T \cdot \delta_k)^{1/2}$, where E – Young’s modulus; σ_T – calculated value of hardening; δ_k – value of critical crack opening, obtained on the basis of substructure parameter data.

The analytical assessment of the mechanical properties of the welded joints made in steel 14HGN2MDAFB in relation to the welding rate revealed that the greatest contribution to the hardening of metal ($\Sigma\sigma_T$) and the increase in brittle crack resistance (K^*_{IC}) was that of the substructure of lower bainite obtained at a rate of 11 mm/s (Fig. 10a). A significant decrease (4 ... 5 times) of indicator K^*_{IC} was characteristic of the minimum welding rate amounting to 5 mm/s, which led to a brittle intergranular crack along the fusion line (Fig. 10c).

The comparison of the change in the calculated value of yield point ($\Sigma\sigma_T$) revealed the phenomena described below. At a welding rate of 5 mm/s, in the weld metal and in the HAZ the calculated value $\Sigma\sigma_T$ amounted to 664 MPa and 859 MPa respectively, the maximum contribution to a yield point was made by substructural $\Delta\sigma_{SG} = 262 - 302$ MPa, dispersive $\Delta\sigma_{D.H.} = 58 - 172$ MPa and dislocation $\Delta\sigma_D = 96 - 150$ MPa precipitates. As regards a welding rate of 11 mm/s, the total value of the yield point grew to 741 - 890 MPa (Fig. 11a). This resulted from the increased

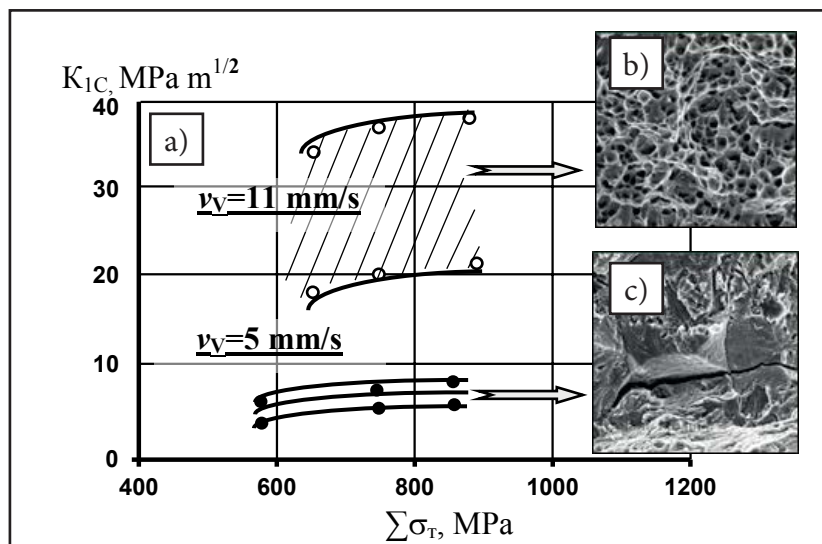


Fig. 10. Change in calculated values of resistance ($\Sigma\sigma_T$) and the critical stress intensity coefficient (K^*_{IC}) in relation to the weld metal (a) and fractographs of plastic failure at a welding rate of 5 mm/s (b); intergranular brittle crack at a welding rate of 11 mm/s (c), $\times 2020$

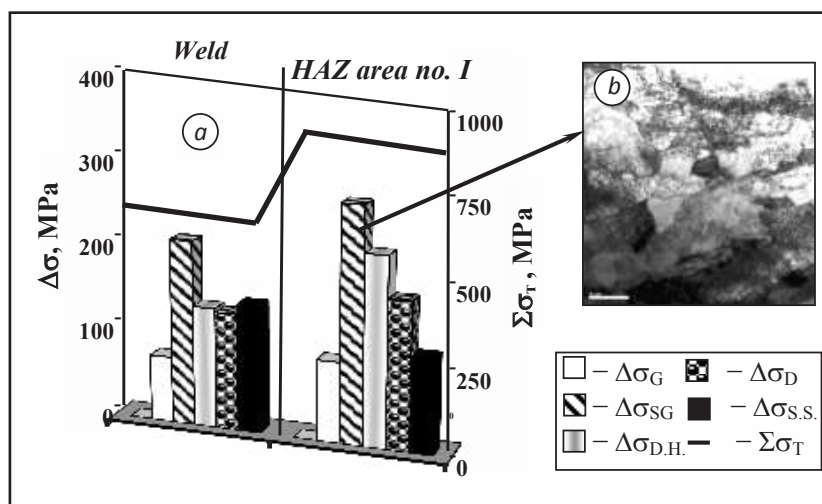


Fig. 11. Contents of various constituents $\Delta\sigma$ of structural hardening in the calculated value of hardening $\Sigma\sigma_T$ of the weld metal (a) and the subtle structure of lower bainite (b) in relation to a welding rate of 11 mm/s, $\times 35000$ ($\Delta\sigma_G$ – hardening along grain boundaries, $\Delta\sigma_{SG}$ – subgrain hardening, $\Delta\sigma_{D.H.}$ – dispersion hardening, $\Delta\sigma_D$ – dislocation hardening, $\Delta\sigma_{S.S.}$ – hardening in the solid solution)

content of the substructural hardening of the constituent of lower bainite $\Delta\sigma_{SG} = 127 - 188$ MPa and dislocation hardening $\Delta\sigma_D = 136 \dots 171$ MPa. The foregoing was related to the increase of the volumetric content of lower bainite up to $V_d = 45 \dots 60\%$.

Therefore, comparing the hardening effect of forming structures (grain size, bainite lath width, distribution of phase precipitate particles) it was ascertained that, as regards the metal of the welded joints made in steel 14HGN2MDAFB, the increase in a welding rate

from 5 mm/s do 11 mm/s increased the hardening effect of the structure, which was related to an increase in the content of lower bainite (Fig. 11b).

The assessment of changes in internal stresses (τ_j) was performed in accordance with a well-known dependence [15] $\tau_j = G \cdot b \cdot h \cdot \rho / [\pi (1 - \nu)]$; where G – shear module; b – Burgers vector; h – foil thickness (0.2 μm); ν – Poisson ratio; ρ – dislocation density.

The calculation-based assessments of local internal stresses (τ_j), presented in the graphs (Fig. 12), reveal that maximum values $\tau_j = 1900 - 3700$ MPa (Fig. 12a) were observed in the HAZ superheating zone metal (5 mm/s) in the areas of elongated dislocation pile-ups ($\rho = 2 \times 10^{11} \text{ cm}^{-2}$) along the boundaries of upper bainite laths (Fig. 12b). The lowest values, relatively uniformly distributed, amounted to $\tau_j = 1100 - 1470$ MPa (11 mm/s, (Fig. 12c)), which was favoured by the formation of fine-grained and fragmented lower bainite structures (Fig. 12d, e).

Conclusions

1. Determined correlations concerning the effect of a mechanised welding rate on the structure of the weld metal and that of the heat affected zone (HAZ) of welded joints made in high strength steel 14HGN2MDAFB revealed that the increase in a welding rate from 5 mm/s to 14 mm/s was accompanied by the change in the weld metal phase composition from ferritic-bainitic into bainitic-martensitic, an microhardness increase of 30% and the repeated refinement of the grain and subgrain structure.

2. The minimum welding rate (5 mm/s) led to the formation of the gradient structure (in terms of size and microhardness) of upper bainite, which resulted in a decrease in mechanical properties and brittle cracking (cold crack

formation) along the fusion line with secondary cracking along grain boundaries.

3. The highest level of local internal stresses was characteristic of upper bainite with high dislocation density gradients, i.e. microcrack nucleation zones. The maximum density and range of the above-named zones were related to a welding rate of 5 mm/s.

4. The most favourable structure of lower fine-grained bainite in the metal of welded joints was formed when the welding rate amounted to 11 mm/s. This provided the optimum combination of mechanical properties, plasticity and the lack of local stress concentrators (crack initiators).

References

- [1] Шоршоров М.Х., Белов В.В.: *Фазовые превращения и свойства стали при сварке*. Москва: Наука, 1972. p. 220
- [2] Madej K., Jachym R.: *Welding of High Strength Toughened Structural Steel s960QL*. Biuletyn Instytutu Spawalnictwa, 2017, no. 2, pp. 6-16. <http://dx.doi.org/10.17729/ebis.2017.2/1>
- [3] Rózański M., Stano S., Grajcar A.: *Effect of Braze Welding Parameters on the Structure and Mechanical Properties of Joints Made of Steel CPW 800. Part 1: Arc Braze*

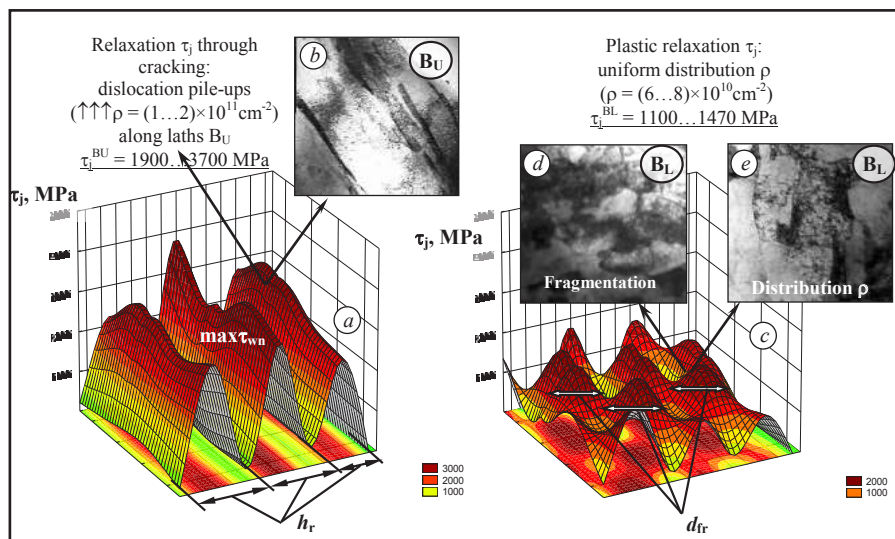


Fig. 12. Distribution of local internal stresses (τ_j) in the structural zones of upper bainite (B_U) obtained at a welding rate of 5 mm/s (a, b) and in the structural zones of lower bainite (B_L) obtained at a welding rate of 11 mm/s (c, d, e), $\times 35000$

- Welding*. Biuletyn Instytutu Spawalnictwa, 2016, no. 6, pp. 6-12.
<http://dx.doi.org/10.17729/ebis.2016.6/1>
- [4] Madej K., Świdergoł S., Jakubiec P.: *Analysis of Cracks in Welded Joints of Pipes with Eyes made of s890QL1 Steel*. Biuletyn Instytutu Spawalnictwa, 2015, no. 6, pp. 11-22.
<http://dx.doi.org/10.17729/ebis.2015.6/2>
- [5] Мусяченко В.Ф., Миходуй Л.И., Жданов С.Л. и др.: *Структурные превращения стали 14ХГНМД при сварке и их влияние на свойства соединений*. Автоматическая сварка. 1985, no. 4, pp. 10-14, 18.
- [6] Маркашова Л.И., Григоренко Г.М., Позняков В.Д., Бердникова Е.Н., Алексеенко Т.А.: *Влияние термических циклов сварки и внешнего нагружения на структурно-фазовые изменения и свойства соединений стали 17Х2М*. Автоматическая сварка. 2009, no. 7, pp. 21-29.
- [7] Маркашова Л.И., Позняков В.Д., Алексеенко Т.А., Бердникова Е.Н., Жданов С.Л., Кушнарева О.С., Максименко А.А.: *Влияние легирования швов на структуру и свойства сварных соединений стали 17Х2М*. Автоматическая сварка. 2011, no. 4, pp. 7-15.
- [8] Позняков В.Д., Маркашова Л.И., Максименко А.А., Бердникова Е.Н., Алексеенко Т.А., Касаткин С.Б.: *Влияние циклического нагружения на микроструктуру и хладостойкость металла ЗТВ стали 10Г2ФБ*. Автоматическая сварка. 2014, no. 5, pp. 3-11.
- [9] Маркашова Л.И., Григоренко Г.М., Бердникова Е.Н.: *Структурные условия оптимизации свойств прочности, пластичности, трещиностойкости сварных соединений*. // Математическое моделирование и информационные технологии в сварке и родственных процессах: Сб. докладов пятой международной конференции (пос. Кацевели, Крым, 25-28 мая 2010 г.). Под ред. проф. В.И. Махненко. Киев: Международная ассоциация «Сварка», 2010, pp. 105-110.
- [10] Гольдштейн М.И., Литвинов В.С., Бронфин Б.М.: *Металлофизика высокопрочных сплавов*. М.: Металлургия, 1986, p. 307
- [11] Конрад Х.: *Модель деформационного упрочнения для объяснения влияния величины зерна на напряжение течения металлов, Сверхмелкое зерно в металлах*. Под ред. Гордиенко Л.К. Москва: Металлургия, 1973, pp. 206-219.
- [12] Petch N.J.: *The Cleavage Strength of Polycrystals*, *Journal of the Iron and Steel Institute*. 1953, V. 174, no. 1, pp. 25-28.
- [13] Келли А., Р. Николсон.: *Дисперсное твердение*. Москва: Металлургия, 1966, p. 187
- [14] Романив О.Н.: *Вязкость разрушения конструкционных сталей*. Москва: Металлургия, 1979, p. 176
- [15] Панин В.Е., Лихачев В.А., Гриняева Ю.В.: *Структурные уровни деформации твердых тел*. Сибирское отделение: Наука, 1985, p. 251